Received June 1999
Revised January 2000
Accepted January 2000

Fluid flow and heat transfer mechanisms in the spray deposition of tubular preforms

T.P. Sperring, J.O. Medwell and D.T. Gethin
Department of Mechanical Engineering, University of Wales, Swansea, UK

Keywords *Heat and fluid flow, Heat transfer, Spray deposition*

Abstract *A combined experimental and numerical investigation into the fluid flow and heat transfer processes that take place in the spray deposition of tubular preforms is presented. The work is concerned principally with impingement mechanisms at jet diameter to target distances that are large in comparison with previous reported studies. The experimental investigation required the design of a novel heat transfer meter that was capable of resolving the heat transfer coefficient within 2.5 per cent. The experiments gave a new correlation for stagnation heat transfer, similar in form to correlations that have been published for small jet diameter to target distance values. The experiments also showed the presence of skewing of the heat transfer coefficient in the deposition zone due to its tapered nature. A finite volume based model of the deposition chamber was developed and run to compare with the experimental data. This model was found to yield trends similar to those measured experimentally, thus confirming its qualitative capability. However the absolute values of heat transfer coefficient that were computed were significantly lower than measured values. This points to the requirement to consider alternative computing schemes and to investigate the methods of representing the heat transfer mechanisms at the physical boundaries, particularly at the preform surface.*

Nomenclature

C_p	= specific heat	T	= temperature
$C_{1\varepsilon}$	= constant in the turbulence dissipation equation	d	= jet diameter
		g_i	= acceleration in direction i
$C_{2\varepsilon}$	= constant in the turbulence dissipation equation	k	= turbulence energy
		p	= pressure
C_μ	= coefficient in the turbulent viscosity equation	u_i	= velocity component i
		x_j	= coordinate direction j
E	= energy	ε	= turbulence dissipation
F_i	= body acceleration contribution	σ	= collision diameter
G_k	= rate of production of turbulent energy	σ_k	= turbulence energy Prandtl number
		σ_ε	= turbulence dissipation Prandtl number
J	= heat flux		
K	= thermal conductivity	μ_t	= turbulent viscosity
L	= jet to target distance	ρ	= density
M	= molecular weight	Ω_μ	= reduced collision integral
R	= gas constant	Nu	= Nusselt number
R_o	= universal gas constant	Re	= Reynolds number

International Journal of Numerical Methods for Heat & Fluid Flow, Vol. 10 No. 3, 2000, pp. 268-285.

The authors wish to acknowledge the financial support of the EPSRC and Osprey Metals Ltd who provided a Case studentship for the first author.

Introduction

Spray forming is a process that is used for the manufacture of high performance near net shape stock materials (Wood, 1990; 1993). The high performance is facilitated by the precise control of cooling to promote a fine microstructure or the inclusion of ceramic fibre to form metal matrix composites. The process is capable of generating preform shapes such as round billets, discs and tubes.

The adaptation that is used in the production of circular tube preforms is shown in Figure 1. The basic stock is melted in an induction furnace and the liquid is controlled to flow at a constant rate through a gas atomiser system. By means of the gas jet, the metal droplets are propelled towards the substrate on which they adhere provided that their condition is appropriate. The preform is subjected to simultaneous rotation and withdrawal and the spray is constrained to scan over the deposition zone.

The parameters that influence the process are shown in Figure 2 (Lawley *et al.,* 1990). This figure confirms the critical importance of the temperature profile through the preform and the independent process parameters associated with heat extraction.

The realisation of appropriate cooling rates is dependent on the spray condition at deposition together with the convective heat transfer mechanisms that are present at the preform surface. The current work is concerned with the heat transfer at the preform surface and this will be investigated using both experimental and numerical modelling strategies.

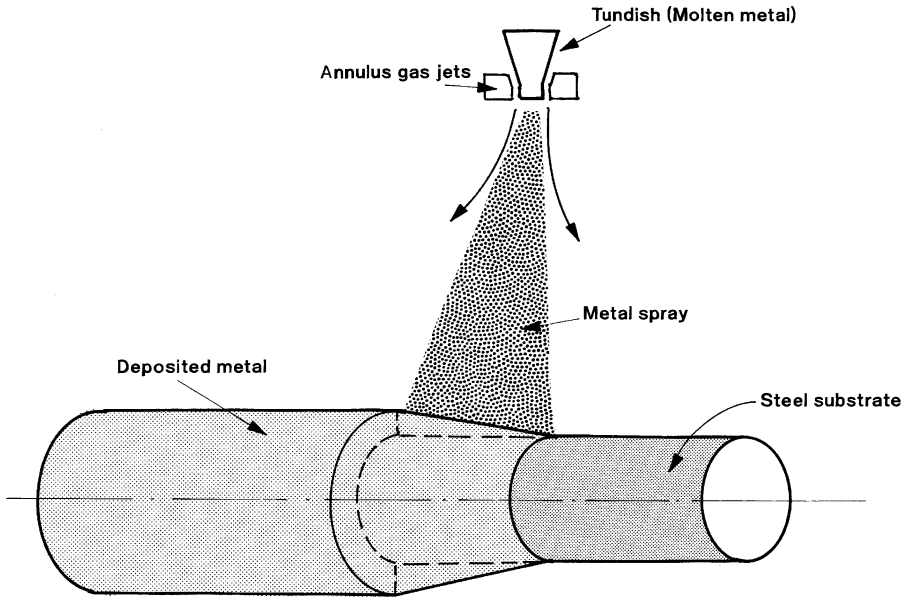

Figure 1.
Schematic of the Osprey tube preform process

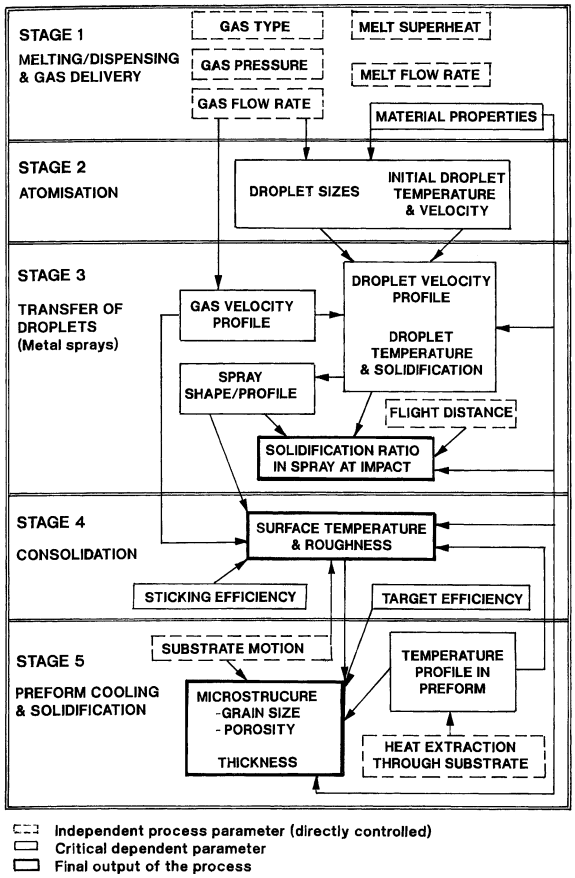

Figure 2.
Flowchart depicting the linking of independent and dependent process parameters during the five stages of the Osprey process (Lawley *et al.*, 1990)

Previous work

Only a very limited amount of work has been published previously that is directly relevant to the heat transfer mechanisms that are present in the spray deposition process (Medwell *et al.*, 1993). This work was concerned with heat transfer in the case of a plain cylindrical preform and used a combination of experimental and numerical techniques to establish an insight to the physical behaviour taking place. The experimental work was conducted by directing an air jet on a heated tube in an open environment. The results demonstrated the high level of heat transfer at the tube surface that is associated with the impingement mechanism. The numerical scheme was found to be capable of yielding qualitatively similar results to those measured experimentally. In this study, this discrepancy was attributed to the complexity of the flow field and the turbulence models that were embodied in the solution procedure.

The other work that has been reported in the literature that is relevant is associated with either modelling or experimental studies on systems that are

closely similar. These focus on impingement heat transfer processes. A selection of these previous studies will be reviewed separately in the following sections.

Experimental investigations

As indicated above, the most relevant work is concerned with jet impingement and convective losses from cylinders in cross flow. Strictly the preform process involves a two-phase system and the fluid motion is induced by a localised jet as opposed to a general flow field. Also the atomisation process leads to extreme gas velocities (Donaldson and Snedeker, 1971) and the target distance to jet diameter is large, typically 50:1.

The high pressures that are required for successful atomisation using a convergent nozzle can lead to supersonic flow at the atomisation point. The work described in Donaldson and Snedeker (1971) leads to different flow regimes dependent on the pressure ratio that is present across the nozzle. At high pressure ratios, an underexpanded jet forms and the flow becomes supersonic. However beyond the atomisation zone, the momentum exchange with the molten metal together with entrainment of surrounding, near stagnant air leads to a large reduction in the gas velocity and an exponential form of decay as the two phase mixture traverses from the atomisation region to the deposition zone. Similarly by means of the momentum exchange and gravitational effects, the metal drops are accelerated towards the target substrate and cooled simultaneously on their trajectory. The latter two phase systems have not been investigated extensively with the most relevant work being associated with atomisation studies (Dombrowski and Johns, 1963). In this work, the authors were concerned with predicting droplet size. They based their model on the interaction between pressure, surface tension, viscous and inertial forces. For a wax type spray, this model consistently predicted droplet sizes that were larger than those measured experimentally and this was attributed in part to the position at which droplets were sampled in the spray.

After the particle laden jet has impinged on the cylinder surface and considering the extreme cases, either it flows laterally along the cylinder leading edge or it flows circumferentially around its surface. The former leads to a wall jet behaviour and the latter to the Coanda effect where the flow adheres to the surface as opposed to separating as it would in the case of a cylinder in crossflow. This is a well known phenomenon and is very likely to have a direct impact on the heat transfer that takes place around the cylinder.

With regard to heat transfer, the most relevant work has been concerned with gas jets impinging normally onto a flat target surface and many studies have been reported in the literature. The main aims of these types of investigation were to examine the heat transfer rates under the impinging jet under different flow conditions and establish the optimum target distance to jet diameter ratio. It was found that this usually lies in the range 6:1 to 8:1 (Hyrcak, 1983). The benefits to be derived from impingement mechanism are substantial with up to an order of magnitude increase in the stagnation point heat transfer

coefficient in comparison with those that are typical in plain convection. However the target distance to jet diameter is not relevant for the spray forming process. Furthermore the tests have not been performed in a chamber environment. Because the cooling rate of the preform is determined mainly by the heat transfer coefficients, this provides one of the motivations for this work.

Numerical modelling

During the last 25 years there has been a great deal of research work published concerning turbulent single phase flow. In this period, solution strategies have become more robust and efficient accounting for the turbulent behaviour by means of a number of models (Nallasamy, 1985).

These schemes have also been applied to two phase flow. For example, the work in Aihara *et al.* (1990) is concerned with mist or droplet cooling processes, highlighting its effectiveness in enhancing heat transfer. Such a mechanism is not relevant in the present problem since the metal phase in the jet transports heat to the substrate which is then removed by the gas phase flow over its surface. The scheme has also been applied to the spray deposition process (Rogers and Katgerman, 1989) where the flow in the chamber was represented as a three dimensional model and the spray was assumed to comprise spherical particles. The purpose of the investigation was to model the trajectory and thermal history of the metal droplets. This can be used to investigate the requirements for powder production, or to establish the thermal condition of the droplet at the point of deposition. The study highlighted the effect of gas pressure and particle size distribution, it focused on the droplets and excluded a consideration of the exchanges that take place at the preform surface.

The work described in Cheng *et al.* (1993) was concerned with investigating the physical behaviour in the deposition process. This included particle size and mass flux in the spray, sticking efficiency and substrate microstructure. The impact of process parameters and spray condition was investigated and this work suggests that ideally the metallic phase should be 30 per cent wet to ensure a high preform density and fine grain size. According to Figure 2 this is controlled most conveniently by the distance between the atomisation point and the substrate.

Lumped parameter type models have also been used to represent the gas and metal phases in the deposition process (Gethin *et al.,* 1990). This calculation is significantly less demanding than that used in Rogers and Katgerman (1989), but it still captures the key mechanisms in the chamber. The extension of these techniques to model the thermal history in the preform has received very little attention. The work described in Forrest *et al.* (1993) is the most relevant in which the authors describe their technique to model the thermal history in a number of preform shapes. However to retain its direct relevance, this model requires the prescription of boundary conditions that represent the behaviour in the spray chamber and to date it has not been possible to specify these based on chamber measurements.

The current review has confirmed that only limited work has been undertaken in connection with fluid flow and heat transfer in the spray forming process. This is a key issue as far as the development and predictability of the process is concerned, motivating the present investigation. This uses both experimental and numerical approaches as described in the following sections.

Experimental investigation

Experimental setup

The focus of the experimental investigation was to establish the heat transfer coefficients over the surface of a tubular preform of the type shown in Figure 1. These measurements need to be local in nature and they need to be performed in a flow field that is appropriate to a deposition chamber. For this reason, a half scale perspex model of a deposition chamber was used and the preform was represented by a wooden form comprising two parallel sections and a taper section where the latter represents the deposit buildup. The arrangement is shown in Figure 3, including the gas supply and measurement systems.

The local heat transfer coefficient can be determined either directly or indirectly. A direct measurement method is described in Sparrow *et al.* (1984) in which the investigator condensed steam onto a plate and measured the temperature gradient through it. The alternative approach is indirect and uses a sublimation analogy to estimate the heat transfer rate (Sparrow *et al.,* 1984). Neither of these is practical for the current investigation and therefore an alternative approach was developed based around the design of a novel heat transfer meter.

The heat transfer meter that was used in this investigation is shown in Figure 4. It comprises a 0.05mm thick heater element of 338mm^2 and this was mounted onto a carbon fibre base of 1mm thickness. The heater is capable of dissipating up to 10W, and a temperature differential of at least 50°C between the heater and ambient temperature was selected to enable an accurate determination of the heat transfer coefficient. The carbon fibre base was chosen

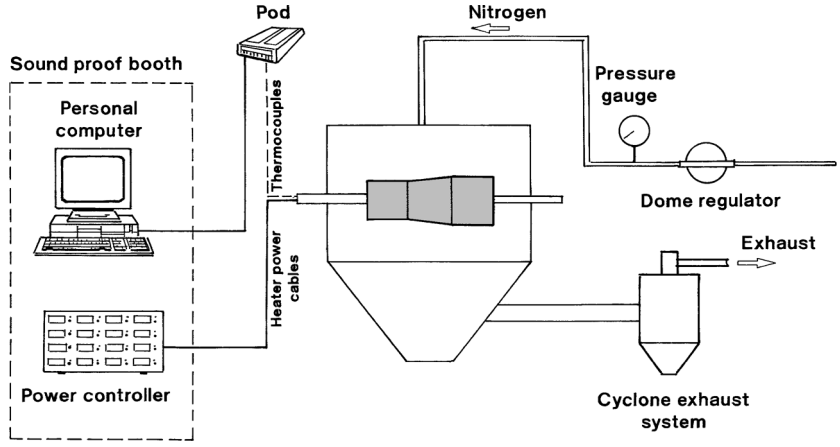

Figure 3.
Schematic of the entire experimental apparatus

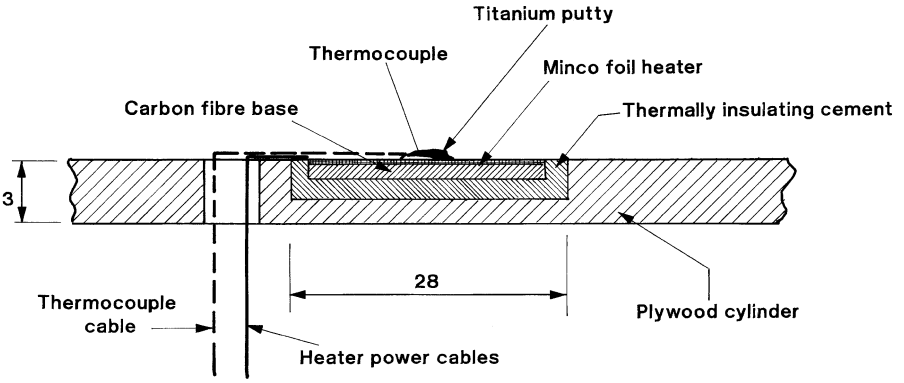

Figure 4.
Heat flux meter design

due to its low thermal conductivity and this was mounted into the preform model using a thermally insulating cement having a conductivity of 0.6W/m°C. This arrangement ensures that all the heat dissipated by the heater flows from its exposed surface. The surface temperature of the heater was measured using type T thermocouples having wires of 0.2mm diameter. These were fixed to the heater surface using titanium putty which has a high thermal conductivity. This was formed to minimise the disturbance to the air flow and the high thermal conductivity ensures that it has minimum impact on the heat transfer from the heater surface.

Each heater had a slightly different resistance and this was measured and accounted for when calculating the dissipation. A single meter was tested initially and was found to be satisfactory in terms of its response speed and measurement capability. Subsequently 15 meters were installed into the wooden former with each connected to an independent power supply and separate data logging channels (Figure 3) where temperatures were recorded within 0.5°C.

Nitrogen was used within the experimental programme and this was supplied to the chamber via a plain sharp edge orifice machined progressively to give holes of 7.0, 8.7 and 10.0mm diameter. This allowed a number of wooden former positions to be investigated at a number of gas supply pressures and the test programme is summarised in Table I. As shown, a number of tests were carried out with the former at one position to investigate the effect of nozzle pressure alone.

	Nozzle diameter (mm)		
Gauge pressure (bar)	7mmϕ	8.7mmϕ	10.0mmϕ
0.686	0° → 180° step 30°	0° → 330° step 30°	0° → 360° step 30°
1.372	0° → 180° step 30°	0° → 180° step 20°	0° → 180° step 30°
2.058	0° → 180° step 20°	0° → 180° step 30°	None
Angular position	Pressure ranges investigated (bar)		
0°	0.34 → 3.45 step 0.34 and 4.12 and 4.81	0.34 → 2.76 step 0.34	0.34 → 2.07 step 0.34

Table I.
Summary of experimental conditions

In the experiments, the gas supply pressure was limited by the structural performance of the perspex chamber. The higher nozzle supply pressure and consequent higher gas flow rate induced sufficient back pressure in the chamber to cause dilation of the sides.

The choice of these conditions allows the heat transfer coefficient to be mapped over the preform surface. During the test, the power supply to each heater was adjusted to ensure a temperature difference of nominally 55°C with respect to the jet chamber temperature. This ensured that the heat transfer data could be measured with sufficient accuracy and that the meters would not be burned out. Using this setup it was possible to measure the heat transfer coefficients within 2.5 per cent.

For the purpose of results presentation the flow through the orifice jet was also calibrated using a volumetric displacement and timing method. This allows the calculation of jet Reynolds number and this was used to display the experimental results.

Experimental results

Figure 5 shows the variation in stagnation heat transfer coefficient over the full range of Reynolds numbers for the three nozzle diameters. The graph confirms the high heat transfer coefficient and that the values are closely similar for the 8.7mm and 10.0mm diameter jets. The slight drop off for the 7.00mm diameter jet is a consequence of a reduction in jet velocity. This was confirmed in separate experiments where it was observed that the velocity profiles for the larger jets were nearly identical whereas the velocity within the smallest jet achieved 70 per cent of their value.

The data for the two larger nozzles were also fitted using non-dimensional groups to give

$$Nu = 1.004\ Re^{0.647}\left(\frac{L}{d}\right)^{-0.773} \quad \text{for } 45 \leq \frac{L}{d} \leq 64 \text{ and } 8 \times 10^4 \leq Re \leq 36 \times 10^4 \quad (1)$$

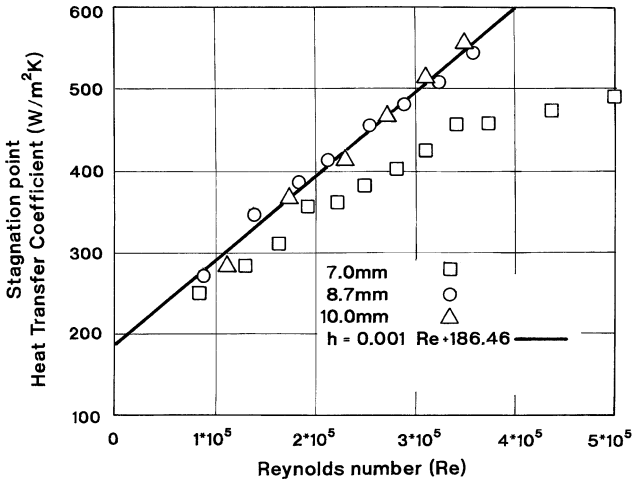

Figure 5.
Stagnation point heat transfer coefficient versus Reynolds number

The results from these experiments may be compared with work published in Mohanty and Tawfeck (1993). Similar trends between stagnation Nusselt and jet Reynolds numbers may be observed. However a dependence on nozzle diameter is also evident with the stagnation value increasing as the nozzle size is increased. The authors did not explain this behaviour and they did not present any information about the fluid velocities. Pertinent to the present study, they established correlations for the three nozzle sizes and the equation for their 7mm diameter nozzle was given as

$$Nu = 0.615\ Re^{\,0.67} \left(\frac{L}{d}\right)^{-0.38} \quad \text{for } 9 \leq \frac{L}{d} \leq 40 \text{ and } 7240 \leq Re \leq 34500 \tag{2}$$

Clearly the range of conditions for the experiments are quite different and the correlation derived in Mohanty and Tawfeck (1993) gives significantly higher Nusselt numbers in comparison with equation 1 under identical conditions where the jet to target distance is small (e.g. $\frac{L}{d} = 9$). However to confirm the levels of Nusselt number, it is appropriate to use the maximum values for Re and $\frac{L}{d}$ in equation (2) since this is closest to the conditions investigated in the present investigation. This yields a Nusselt number of 167 which is now in close agreement with the values that have been derived in the present study. This supports the correlation that is presented in equation (1) for large $\frac{L}{d}$ values that are appropriate in the spray forming process.

Figures 6 and 7 display the circumferential and axial variation of heat transfer under the axis of the jet for the three jet diameters. Results have been presented at one pressure of 0.686b. Data are also available at higher pressures and the form of the distribution is similar in each case with the maximum value increasing as pressure is increased, as explained in connection with Figure 5. The notable feature is that there is no rapid drop off in heat transfer about the back face of the preform. This occurs because the jet does not separate as is the case of a cylinder in uniform cross flow. This is the Coanda effect and it has a clear impact on the heat transfer from the preform surface.

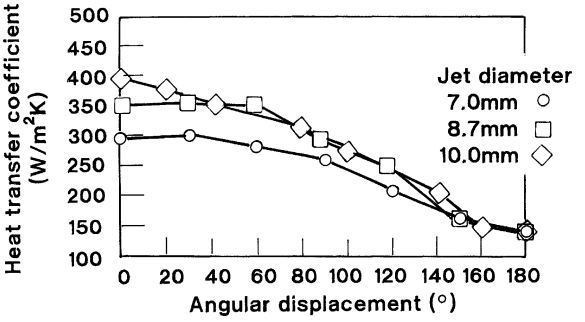

Figure 6.
Circumferential variation of heat transfer coefficient for a nozzle pressure of 0.686 bar

The axial variation in heat transfer coefficient along the cylinder leading edge is shown in Figure 7. It displays similar trends with respect to jet diameter and exhibits a bell shaped profile as presented in Mohanty and Tawfeck (1993). However in this case, the profile displays a small asymmetry with respect to the jet centreline. The heat transfer is marginally higher at the substrate surface (axial position –300mm) in comparison with the preform zone (axial position +300mm). This is a consequence of the air flow deflection over the tapered conical section that represents the build-up of the preform. This information is also presented in a normalised format in Figure 8. The graphs include data from Sparrow and Lovell (1980) that are appropriate for $\frac{L}{d} = 15$ and a jet impinging obliquely onto a flat surface. This figure shows the detail of the increased spread for the lower diameter nozzle and the skewing of the heat transfer over the preform which becomes most noticeable for the larger jet. The increased spread for the smaller nozzle is a consequence of the more marked reduction in jet velocity due to the momentum exchange with the entrained air (Gethin *et al.,* 1990). The more extreme skewing for the largest nozzle is a consequence of the air flow over the sloping section that represents the

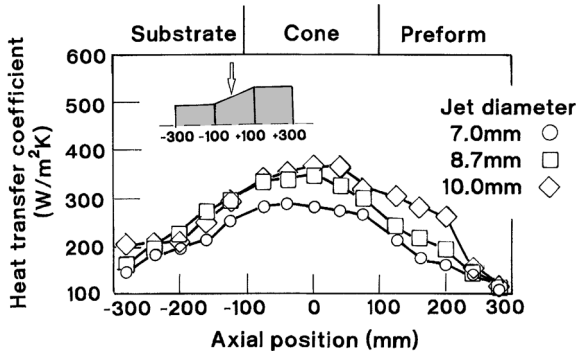

Figure 7.
Heat transfer coefficient for different axial positions for a nozzle pressure of 0.686 bar

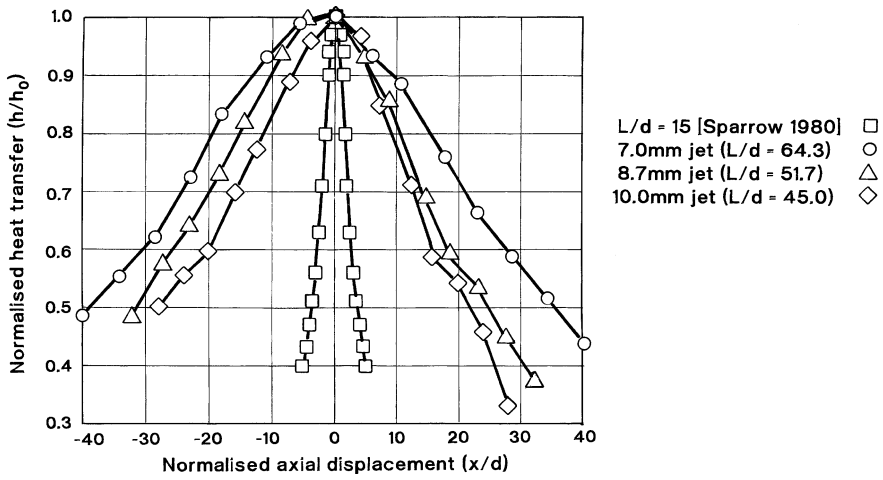

Figure 8.
Variation in normalised heat transfer coefficient with axial position

deposition zone. The spreading of the jet may be compared with the result in Sparrow and Lovell (1980). It is large by comparison and this is also a consequence of the momentum exchange with the entrained air which now takes place over a much larger $\frac{L}{d}$ ratio. However unlike the present study, the results from Sparrow and Lovell (1980) do not display any asymmetry due to the jet impinging obliquely onto the target surface and this may be attributed to the significantly smaller jet diameter. Indeed it may not be possible to detect such skewing when using the sublimation analogy adopted in Sparrow and Lovell (1980) as a technique to measure heat transfer coefficients.

Figure 9 displays the heat transfer coefficient in contour form over half the development of the preform under the jet. The contours are symmetric about the circumferential position under the jet axis and this was confirmed as part of the detailed experimental investigation. The figure displays the region of high

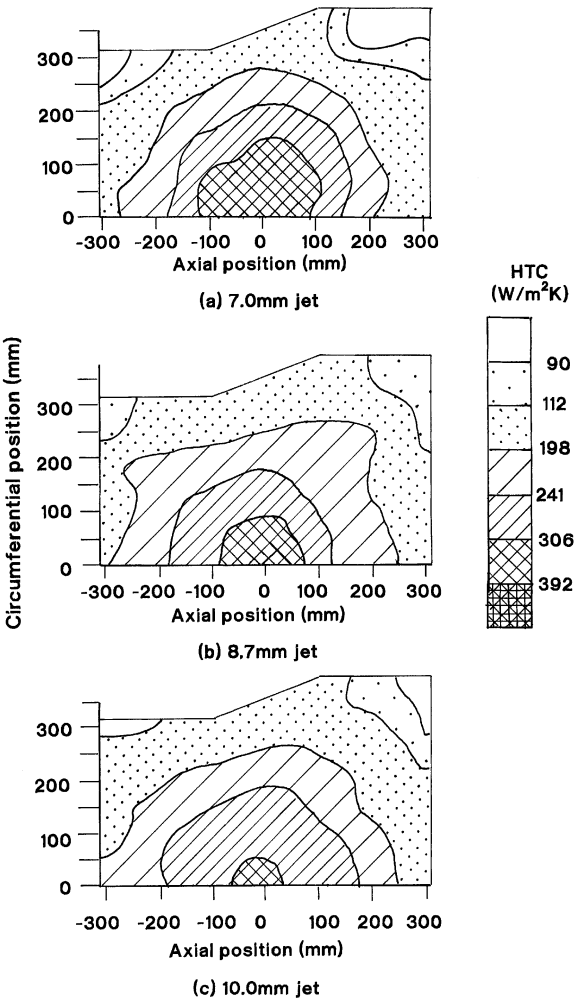

Figure 9.
Heat transfer coefficient contours over the developed preform surface. Nozzle pressure 0.686 bar

heat transfer under the jet axis together with the slight skewing as depicted in Figure 8. Within the zones of maximum heat transfer, the actual maxima achieved cannot be seen clearly. Close examination revealed that for the 7mm jet the maximum value was 306 W/m$^{2\circ}$C, for the 8.7mm jet it was 350 W/m$^{2\circ}$C and for the 10mm jet it was 390 W/m$^{2\circ}$C.

These experimental data will be compared with a numerical model of the deposition chamber and this will be presented in the next section.

Numerical model

A numerical model of the deposition chamber and preform was constructed using a commercial code (FLUENT, 1995). The basis of the numerical scheme is well documented in the literature (Patankar, 1980) and therefore only the governing equations will be presented.

The governing equations comprise mass, momentum, turbulence transport and energy conservation. These are coupled both hydrodynamically and via thermo-physical properties of the fluid. They are written

$$\frac{d\rho}{dt} + \frac{\partial}{\partial x_j}(\rho u_i) = 0 \text{ mass conservation} \tag{3}$$

$$\frac{d}{dt}(\rho u_i) + \frac{\partial}{\partial x_j}\left(\rho u_i u_j\right) = \frac{-\partial p}{\partial x_i} + \frac{\partial \tau_{ij}}{\partial x_j} + \rho g_i + F_i \text{ momentum}$$
$$\text{where } \tau_{ij} = \left[\mu\left(\frac{\partial u_i}{\partial x_j} + \frac{\partial u_j}{\partial x_i}\right)\right] \tag{4}$$

For a two equation turbulence transport model

$$\frac{d}{dt}(\rho k) + \frac{\partial}{\partial x_i}(\rho u_i k) = \frac{\partial}{\partial x_i}\left(\frac{\mu_t}{\sigma_k}\frac{\partial k}{\partial x_i}\right) + G_k + G_b - \rho\varepsilon \tag{5a}$$

$$\frac{d}{dt}(\rho\varepsilon) + \frac{\partial}{\partial x_i}(\rho u_i \varepsilon) = \frac{\partial}{\partial x_i}\left(\frac{\mu_t}{\sigma_\varepsilon}\frac{\partial \varepsilon}{\partial x_i}\right) + C_{1\varepsilon}\frac{\varepsilon}{k}G_k - C_{2\varepsilon}\, p\frac{\varepsilon^2}{k}$$
$$\text{where } \mu_t = \rho\, C_\mu \frac{k^2}{\varepsilon} \text{ and } G_k = \mu_t\left(\frac{\partial u_j}{\partial x_i} + \frac{\partial u_i}{\partial x_j}\right)\frac{\partial u_i}{\partial x_i} \tag{5b}$$

In equation 5, there are five constants that are based on modelling a diverse set of flow scenarios. The best known values were adopted in this work, notably

$$C_{1\varepsilon} = 1.44,\ C_{2\varepsilon} = 1.92,\ C_\mu = 0.09,\ \sigma_k = 1.0 \text{ and } \sigma_\varepsilon = 1.3.$$

For heat transfer, the energy equation may be written as

$$\frac{d}{dt}(\rho E) + \frac{\partial}{\partial x_i}(\rho u_i E) = \frac{\partial}{\partial x_i}\left(K\frac{\partial T}{\partial x_i}\right) - \frac{\partial}{\partial x_i}\sum EJ + \frac{\partial \rho}{\partial t} + u_i\frac{\partial \rho}{\partial x_i} + \tau_{ij}\frac{\partial u_i}{\partial x_j} \tag{6}$$

The details of the flow and heat transfer adjacent to physical boundaries was captured by means of wall functions (Launder and Spadling, 1973) since this eliminates the need for grid refinement adjacent to physical boundaries for the sole purpose of capturing the details in the boundary layer. This reduces the computational requirements in this region.

Noting that Nitrogen is a monatomic gas, the variation of thermo-physical properties was expressed via the equations.

$$\rho = \frac{p}{RT} \quad \text{density} \tag{7}$$

$$\mu = 2.67 \times 10^{-6} \quad \frac{\sqrt{MT}}{\sigma^2 \Omega_\mu} \quad \text{viscosity} \tag{8}$$

$$k = \tfrac{15}{4} \cdot \frac{R_o}{M}\, \mu \left(\frac{4}{15}\, \frac{C_p M}{R_o} + \frac{1}{3}\right) \quad \text{thermal conductivity} \tag{9}$$

$$\text{and } C_p = \frac{5}{2} \cdot \frac{R_o}{M} \quad \text{specific heat capacity} \tag{10}$$

These equations are general and are based on molecular considerations (Hirschfelder *et al.,* 1954). For the purpose of the present work, the values from these equations were checked against tabulated data for Nitrogen and they were found to be appropriate.

In developing the models, initially two dimensional sections were used to investigate computational demands and to perform some mesh sensitivity studies. This allowed progress to the three dimensional model that uses body fitted co-ordinates as shown in grid form in Figure 10. The grid captures the preform geometry, chamber baffle plates and exhaust ports. The grid becomes

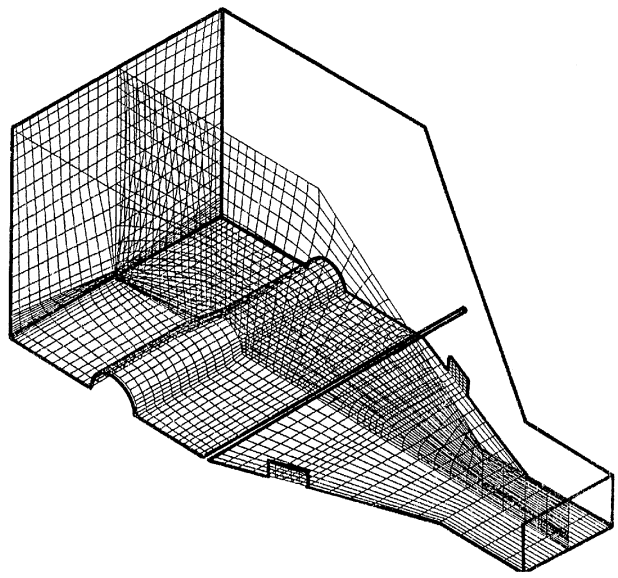

Figure 10.
Isometric view of the three dimensional grid

fine and concentrated at the jet since this needs to approximate the jet immediately down stream from the atomisation zone. This grid comprises 41,325 cells.

For this model, wall conditions were applied at physical boundaries and outlet zones at the exhaust ports from the chamber. The jet geometry was chosen to suit the 10mm diameter jet and inlet velocities from 100m/s to 400m/s were investigated in this study. These were chosen to represent appropriate extremes of jet velocity where the latter is effectively supersonic due to the under-expanded nature of the jet in the atomising region.

The thermal boundary conditions that were used approximate the experimental set up, notably chamber wall temperatures of 0°C and a preform temperature of 27°C. The main requirement is that the latter is sufficient to allow the accurate calculation of heat transfer at the surface based on wall temperature and the temperature within the cell adjacent to the wall. The gas supply temperature was also set at 0°C. These conditions do not represent the conditions within the deposit chamber where temperatures are substantially higher. Earlier calculations used chamber conditions and it was found that under these more extreme circumstances, the nonlinear effects that were introduced via thermophysical properties made it difficult to obtain a converged solution. Thus the conditions that have been used are purely for the purpose of investigating the variation in heat transfer coefficient over the preform surface. Thus these results may be compared directly with the experimental programme that was described in the preceding section.

The decay in velocity along the jet axis is shown in Figure 11. The decay is a consequence of air entrainment and it adopts the expected inverse function with respect to distance from the nozzle. Clearly the velocity at the preform surface is zero. However for the highest inlet velocity of 400 m/s there is a very

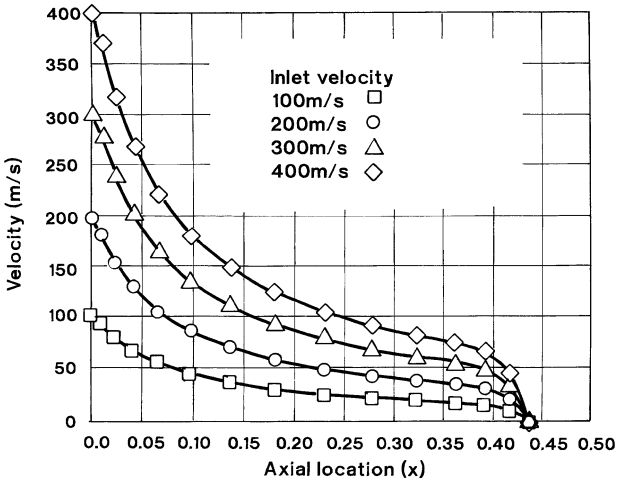

Figure 11. Velocity decay between the nozzle and target for a 10mm diameter jet

sharp deceleration adjacent to the preform. This higher level of impingement velocity has a major impact on the heat transfer and this will be discussed further in connection with Figures 12 and 13.

The heat transfer from the preform was computed and its circumferential and axial variation is presented in Figures 12 and 13. The form of the profile together with its variation with jet velocity demonstrates the expected trends with regard to the experimental work as discussed in connection with Figures 5 and 6. Close examination of Figure 12 and its comparison with Figure 6 shows differences in level and detail. Clearly the stagnation heat transfer coefficient is significantly lower and the predicted value shows a noticeable peak up to 40° either side of the stagnation line. The general form around the preform surface is correct and an examination of the flow field confirmed that the flow adhered

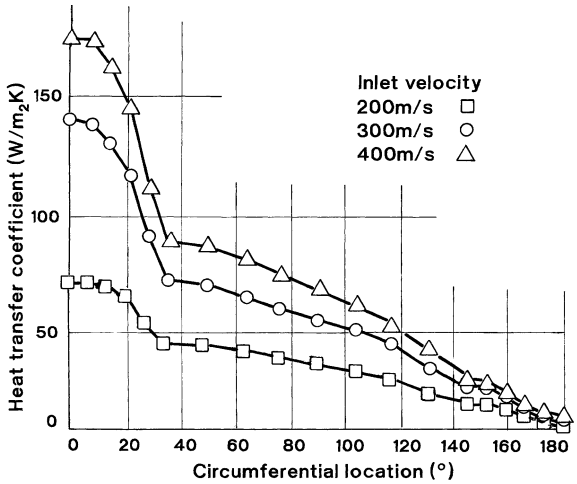

Figure 12.
Circumferential variation in heat transfer coefficient

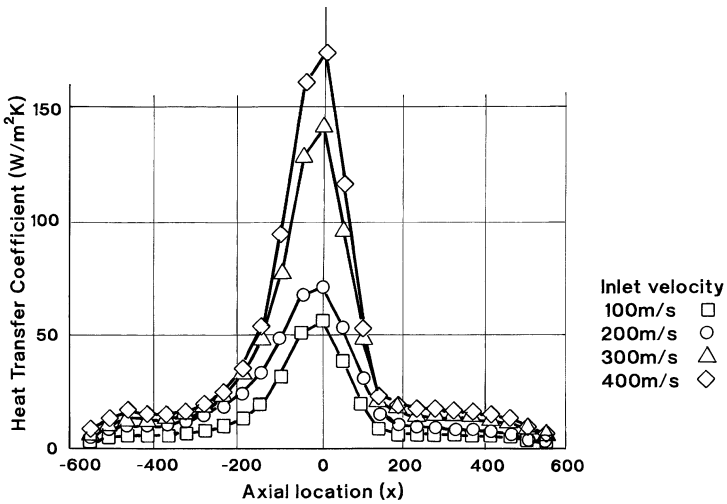

Figure 13.
Axial variation heat transfer coefficient

to the preform surface as a consequence of the jet flow and the adjacent walls of the spray chamber. However the low level of heat transfer coefficient suggests that even if the form of the flow field is correct, the magnitude is not. This was also observed in the work reported in Medwell *et al.* (1993). This points to the requirement to develop the modelling further, possibly by investigating alternative methods to capture the local nature of the heat transfer details in the boundary layer, or possibly by accounting for the compressible nature of the flow. Each of these will require algorithm developments and possibly the application of different numerical techniques, such as the finite element method. Figure 13 shows the axial variation of heat transfer coefficient and this demonstrates the expected variation with respect to nozzle velocity. A more direct comparison is shown in Figure 14. The curves show that the model predicts correctly the skewing of the heat transfer as a consequence of the flow induced by the tapered section of the preform.

Finally, Figure 15 displays the predicted heat transfer contours over the preform with experimental data overlaid. This confirms the correct qualitative prediction of the numerical model. However as elaborated above, it clearly under-predicts the absolute level of heat transfer within the chamber.

Conclusions

A combined experimental and numerical investigation into the fluid flow and heat transfer behaviour in deposition chamber used in the spray forming process has been presented.

It may be concluded that the experimental work has established a simple heat flux meter to measure local heat transfer coefficients and this has been applied to establish the coefficients over the preform surface. The heat transfer data that have been recorded are appropriate for jets having large target distance to nozzle diameter ratios and this represents a new contribution to the literature. These results give stagnation Nusselt number correlations that are

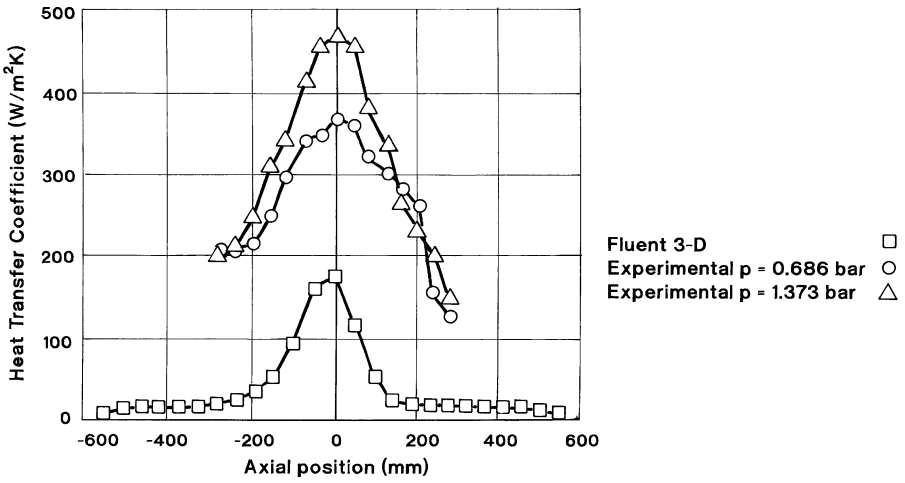

Figure 14.
Comparison of axial heat transfer coefficient results

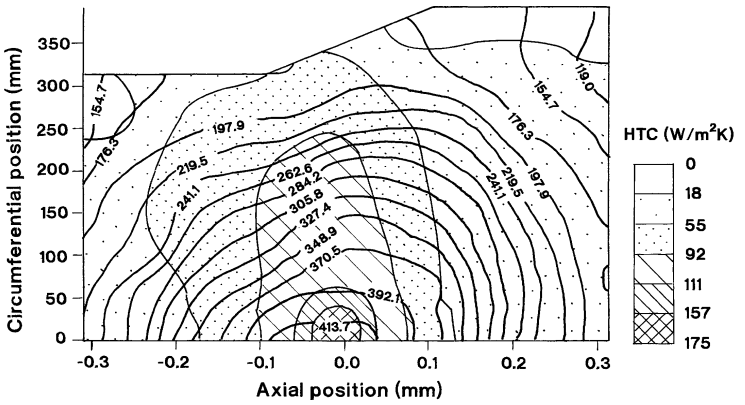

Figure 15.
Comparison of heat transfer coefficient contour map, jet velocity 400m/s

similar in form to those from experiments on jets having low $\frac{L}{d}$ ratios. When impacting on to the preform, the jet adheres to the preform surface and there is no step reduction in the heat transfer coefficient as a consequence. Finally the tapered section deflects the airflow and introduces a skew into the heat transfer rates that is most affected for the larger jet diameter.

A three dimensional numerical simulation of the chamber was found to be capable of capturing the form of the flow pattern in the chamber and heat transfer variation over the preform surface. The scheme was not capable of capturing the actual values of heat transfer coefficient and consistently underestimated the measured values by a factor of approximately 2.5. This points to the need to develop more accurate numerical schemes. Possible avenues to achieve this will be to include the compressibility of the flow and to model the heat transfer at the preform surface in a more rigorous manner.

References

Aihara, T., Fu, W.S. and Suzuki, Y. (1990), "Numerical analysis of heat and mass transfer from horizontal cylindrical downward flow of air – water, mist" *ASME Journal of Heat Transfer*, Vol. 112, pp. 472-8.

Cheng, C., Annavarapu, S. and Doherty, R. (1993), "Modelling – based microstructure control in spray casting", *Second International Conference on Spray Forming*, 13-15 September edited by J.V. Wood, Woodhead, Cambridge, pp. 67-83.

Dombrowski, D. and Johns, W.R. (1963) *Chemical Engineering Science*, Vol. 18, pp. 203-14.

Donaldson, C.D. and Snedeker, R.S. (1971), "A study of free jet impingement, part 1", *Journal of Fluid Mechanics*, Vol. 45, pp. 281-319.

FLUENT, Version 4.3, FLUENT Incorporated, 1995.

Forrest, J., Lile, S. and Coombs, J. (1993), "Numerical modelling of the Osprey process", *Second International Conference on Spray Forming*, , 13-15 September edited by J.V. Wood, Woodhead, Cambridge, pp. 117-27.

Gethin, D.T., Medwell, J.O. and Muhamadi, N. (1990), "A comparison of lumped parameter techniques for liquid metal sprays", *First International Conference on Spray Forming*, 17-19 September edited by J.V. Wood, Woodhead, Cambridge.

Hirschfelder, J.O., Curtis, C.F. and Bird, R.B. (1954), *Molecular Theory of Gases and Liquids*, J. Wiley, New York, NY.

Hyrcak, P. (1983) "Heat transfer from a round impinging jet to a flat plate", *International Journal of Heat and Mass Transfer*, Vol. 26, pp. 1857-65.

Launder, B.E. and Spadling, D.B. (1973), "The numerical computation of turbulent flows", Imperial College of Science and Technology, NTIS 1074-14066.

Lawley, A., Mathur, P., Apelian, D. and Meystel, A. (1990), "Spray forming: process fundamentals and control", *Powder Metallurgy*, Vol. 33, pp. 109-11.

Medwell, J.O., Gethin, D.T. and Wismakumara, A. (1993), *Heat Transfer Phenomena in the Osprey Preform Process, Second International Conference on Spray Forming*, 13-15 September edited by Wood, J.V., Woodhead, Cambridge, pp. 85-104.

Mohanty, A.K. and Tawfeck, A.A. (1993), "Heat transfer due to a round jet impinging normal to a flat surface", *International Journal for Heat and Mass Transfer*, Vol. 36, pp. 1639-47.

Nallasamy, M. (1985), "A critical evaluation of various turbulence models as applied to internal fluid flows" NASA Paper 2474.

Patankar, S.V. (1980), *Numerical Heat Transfer and Fluid Flow*, Hemisphere Publishing Corporation, Washington, DC.

Rogers, S. and Katgerman (1989), "Particle tracking of solidifying molten metal droplets during gas phase atomisation", in Lewis, R.W. and Morgan, K. (Eds), *Proc. Numerical Methods in Thermal Problems*, pp. 1580-90.

Sparrow, E.M. and Lovell, B.J. (1980), "Heat transfer characteristics of obliquely impinging circular jet", *ASME Journal of Heat Transfer*, Vol. 102, pp. 202-9.

Sparrow, E.M., Altermani, C.A.C. and Chaboki, A. (1984), "Jet impingement heat transfer for a circular jet impinging in crossflow on a cylinder", *ASME Journal of Heat Transfer*, Vol. 106, pp. 570-7.

Wood, J.V. (1990) (Ed.), *First International Conference on Spray Forming*, 17-19 September, Woodhead, Cambridge.

Wood, J.V. (1993), *Second International Conference on Spray Forming*, 13-15 September, Woodhead, Cambridge.